Nonlinear modeling parameters and acceptance criteria for concrete columns

Ghannoum, W. M., Matamoros, A. B.

Abstract

A database of 490 pseudo-static tests of reinforced concrete columns subjected to load reversals was used to evaluate nonlinear modeling parameters that define the lateral force versus lateral deformation envelope relation of columns under seismic excitations. Based on the modeling parameters, criteria that identify acceptable deformation levels at various performance objectives are proposed. The effects of bi-directional loading and number-of-cycles of the displacement history on the drift ratio at axial failure are discussed, and recommendations are given to account for such effects. Modeling parameters and acceptance criteria are provided in a format that is consistent with provisions of the ASCE 41-06 Standard entitled "Seismic Rehabilitation of Existing Structures".

Keywords: concrete, columns, nonlinear, modeling parameters, acceptance criteria, bi-directional, cyclic, seismic

1. Introduction

When estimating the performance of existing structures subjected to seismic events, it is often necessary to conduct nonlinear dynamic analyses that require the definition of the lateral force versus lateral deformation relation of frame members. Based on a database comprised of 490 reinforced concrete column tests [1, 2], relations are proposed to define key limiting deformations in the lateral force-deformation relation of reinforced concrete columns subjected to seismic demands. More specifically, relations for evaluating plastic rotations at incipient lateral-strength degradation and incipient axial degradation are proposed. Furthermore, recommendations are provided for selecting acceptable deformations or Acceptance Criteria (AC) below which the performance of reinforced concrete columns is deemed acceptable for selected target performance objectives.

The proposed relations and recommendations are given in a format that is compatible with the standard for seismic rehabilitation ASCE 41-06 Supplement 1 [3, 4]; hereafter referred to as ASCE 41. The standard defines the nonlinear force-deformation backbone relations of concrete columns and other members as illustrated in Fig.1a. In the Figure, the plastic rotation at incipient lateral-strength degradation is given through the Modeling Parameter (MP) *a*. The plastic rotation in a concrete column at incipient axial degradation is given through the MP *b*. The residual lateral strength of a column is given by the MP *c*. MP *a* and *b* are given in the current standard as conservative lower-bound estimates of experimental values (Fig. 1b) [5]. To avoid skewing the results of nonlinear simulations, the proposed MP *a* and *b* will target median experimental values. AC in the standard were based on fixed percentages of the MP for various performance objectives. Because the error on the estimates of MP exhibit different dispersions for various parameters and members, selecting a fixed fraction of those MP values for AC results in varying probabilities of exceedance for the AC (e.g., 75% of a MP does not always provide the same probabilities of exceedance because that probability depends on the standard deviation on the MP estimate) . Thus, proposed AC are defined through fixed probabilities of exceedance for various performance objectives and the corresponding factions of MP values that achieve those probabilities are given.

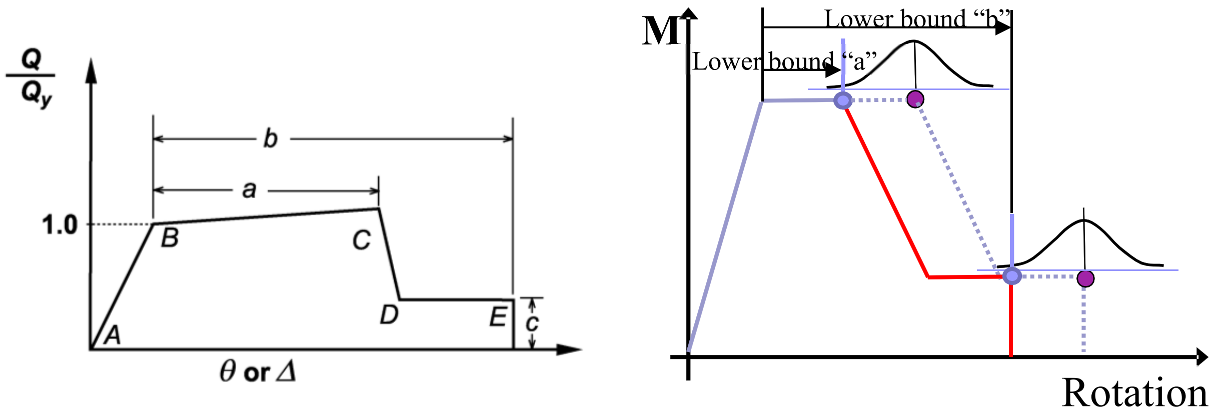

a) b)

Figure 1: a) ASCE 41-06 backbone response for nonlinear modeling of RC components (from [3]); b) illustration of MP deviation from median values and resulting backbone for modeling RC elements.

2. Column Database

The database used to support the development of the proposed MP and AC contains 319 rectangular column tests and 171 circular column tests for a total of 490 tests [1, 2]. Much of the data was derived from the PEER column database [6]. All tests in the database were conducted quasi-statically. The new database is webcast and accessible to the public ([1, 2]) and additional information about the database can be found in Sivaramakrishnan [7]. The distributions of key parameters of the columns in the data sets are illustrated in the bar charts of Fig. 2. Out of the rectangular columns in the database, 37 can be considered to satisfy the requirements of ACI 318-11 [8] for Special Moment Resisting Frames (SMRF). Out of the circular columns, 24 can be considered to satisfy these requirements. A limited number of rectangular columns (25 out of 171) have reported ties with 90^{o} hooks. The tie hook-angle is unknown for 26 rectangular columns, while 269 rectangular columns have ties with 135^{o} hooks or welded ends. A limited number of circular columns had ties with lapped ends (13 out of 171). Tie details were unknown for one circular column, while the remainder of the circular columns had spirals, ties with welded ends, or hooks anchored into the core. Limited information on hook extensions was available for column tests of the database. Splices and anchorage deficiencies are not within the scope of the work presented, and as such no tests on columns containing anchorage deficiencies were used.

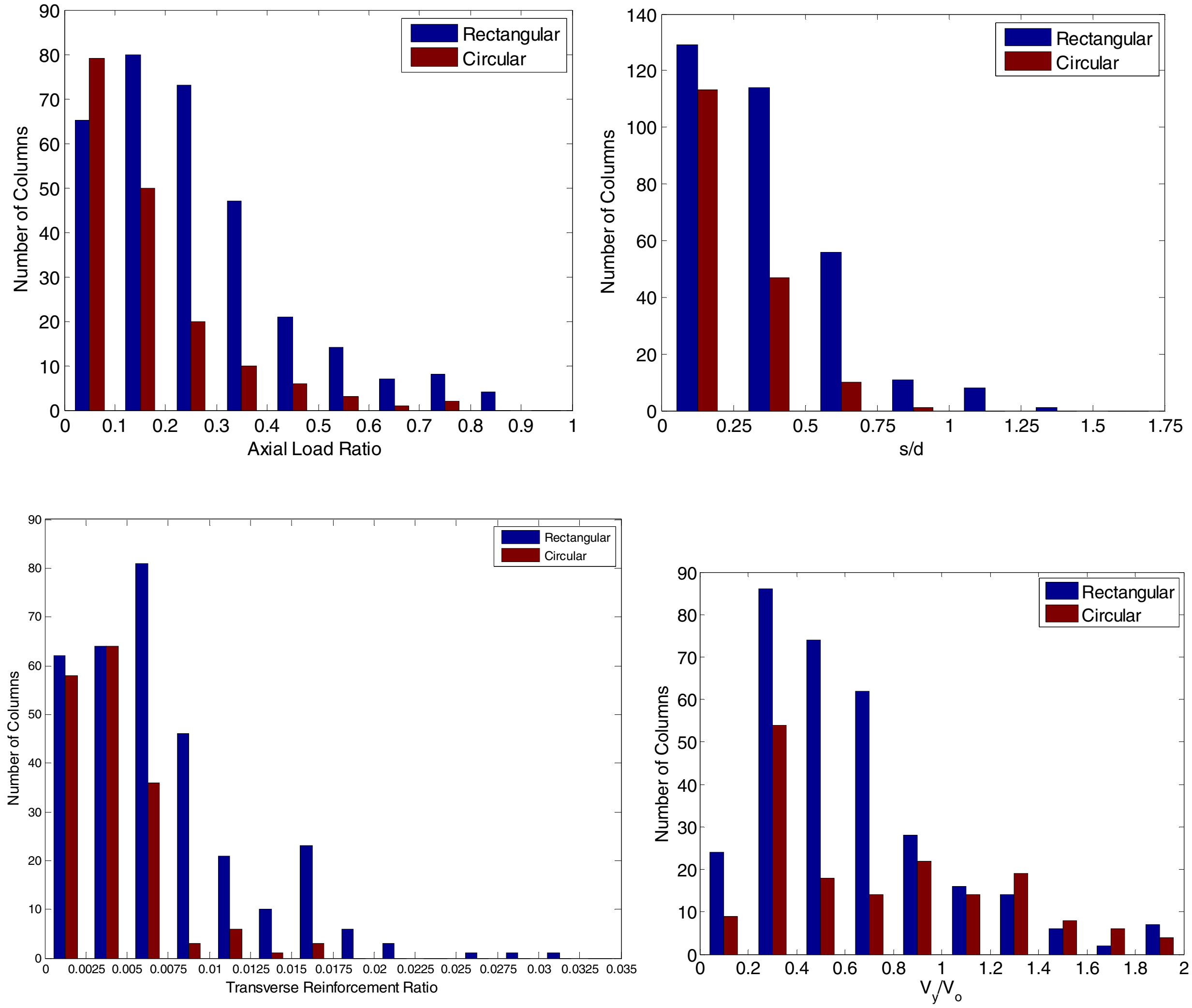

Figure 2: Distribution of key parameters in column database – *see Notation section for term definitions*

3. Data Extraction

The values of *a* and *b* were extracted for all column tests. The *a* values were taken as: $a = (\Delta_{0.8}-\Delta_y)/L$ with $\Delta_{0.8}$ = lateral drift at which the lateral strength of an element degrades by 20% from peak, Δ_y = lateral drift at onset of significant inelastic deformations, and L = column clear length. The drift at onset of inelastic deformation, Δ_y, was obtained as recommended by Sezen and Moehle [9]. A secant line was extended on the lateral force-deformation plot of a column test from the origin to the point on the backbone curve at 70% of the maximum shear (0.7 V_{max}). Δ_y was then taken as the drift at the intersection of the secant line with the horizontal line drawn at V_{max}. Δ_y was also evaluated using a secant line passing through 0.6 V_{max}. Little difference was observed between results from the two intercepts. Results based on a 0.7 V_{max} intercept were used in parameter extractions.

The drifts at yield obtained as described above differ from estimates that would be obtained using column stiffness relations provided in the ASCE 41 standard. ASCE 41 stiffness relations were not used for extracting paraerters *a* and *b* to avoid skewing the extracted plastic rotations by errors in stiffness estimates inherent in the ASCE 41 stiffness relations [10] (especially for columns with low deformation capacities). The objective of the study was to extract the best estimate of plastic rotations *a* and *b* such that the proposed relations defining them would provide median estimates of the plastic rotations and the trends described in those relations would not be artificially altered. The outcome for users of the standard that opt to use ASCE 41 stiffness relations will be a slightly skewed total deformation capacity for elements, but the estimated behavior of the elements would not be skewed (i.e., the degree of inelastic deformations prior to loss of strength estimated by the relations would be the median estimate). Moreover, the proposed relations are intended to be used not only with the ASCE 41 elastic stiffness relations but also with other methods for evaluating stiffness (such as fiber-section models).

Due to the scarcity of column tests conducted to collapse, two sets of *b* values were produced. The first set originates from column tests that were conducted to axial collapse. If a test was conducted to axial collapse, the plastic rotation at axial failure was taken as $b_1 = (\Delta_{axial}\text{-}\Delta_y)/L$; with Δ_{axial} = drift at onset of axial collapse. Only 36 rectangular and 9 circular columns in the database were pushed to axial failure. The webcast database was further bolstered by 12 recent rectangular-column collapse tests [11, 12]. The second set of *b* values, b_2, includes the first set but also introduces *b* values for all other columns in the database based on the following:

- If a test reached a drift at which the lateral strength degraded to 25% of the peak but no axial failure was reported, the plastic rotation at that drift was taken as b_2. This limit on deformations at axial failure was introduced to mitigate possible errors or omissions in the reporting of axial failure in database tests. Columns that lost 75% of their lateral strength were deemed unstable and close to axial collapse.
- If a columns was not tested to collapse or to a deformation causing a reduction in lateral strength to below 25% of the peak lateral strength, the plastic rotation at the largest drift a column was pushed was taken as b_2.

This methodology provides a lower bound estimate on the parameter *b* but utilizes all the available column tests. Additional details about the process by which the plastic rotations were extracted from the database can be found in [7].

Values of V_y were extracted from experimental data through analytical means. In all calculations, measured material properties were used. V_y is defined as the shear demand corresponding to the development of moment strength in a column. $V_y = M_y/L_a$ with M_y = column moment capacity, and L_a = column shear span. M_y was calculated using fiber-section analyses that utilized the parabolic stress-strain relation for concrete proposed by Hognestad [13] for concrete in compression. The limiting strain in compression for the concrete was adopted as 0.003. Confinement effects on concrete material properties, as well as the tensile strength of concrete were neglected. An elastic perfectly plastic material model was used for steel fibers and capped at the measured yield stress of longitudinal bars.

ACI 318-11 specifies the use of the ultimate stress of longitudinal bars (approximated as 1.25 the specified yield stress) when evaluating the flexural strength of plastic hinges in flexural members. The increment of 1.25 on yield stress is an arbitrary limit to ensure that an upper bound estimate of the shear demand is used for proportioning the transverse reinforcement. In the study that was performed, measured values of yield stress were used in calculating V_y for following reasons:

1) In reinforced concrete columns, longitudinal bars will only reach ultimate stress in well confined columns that are pushed to large inelastic deformations. For columns that sustain shear failure prior to flexural yielding or at relatively low inelastic deformations, evaluating V_y using the yield stress of bars is more appropriate.
2) Deriving the modeling parameter and acceptance criteria relations using lower V_y values obtained using the yield stress of bars would provide lower modeling parameters and acceptance criteria should users opt to evaluate V_y using 1.25 the yield stress of longitudinal bars.

The beneficial effects of confinement on flexural strength were not included in calculations of V_y for similar reasons.

V_o was evaluated based on the shear-strength equation of ASCE 41-06 for reinforced concrete columns. The shear strength equation used was:

$$V_o = \Phi \frac{A_v f_{yt} d}{s} + \left(\frac{\alpha\sqrt{f_c'}}{M/Vd} \sqrt{1 + \frac{N_u}{\alpha\sqrt{f_c'} A_g}} \right) 0.8 A_g \qquad \text{Eq. 1}$$

where α = 6 in psi units and 0.5 in MPa units; N_u = axial compression force (= 0 for tension force); M/Vd is the ratio of moment to shear times the effective depth and was bounded by the values of 4 and 2; d is the effective depth; and A_g is the gross cross-sectional area of the column. For circular columns $d = 0.8D$, where D is the diameter of the column. To account for the inefficacy of transverse reinforcement in resisting shear when spaced beyond 75% of the effective depth of a section, the steel contribution to shear strength (first term in Eq. 1) was modified by a factor of Φ that was taken as 1.0 for $s/d \leq 0.75$, zero for $s/d \geq 1.0$, and linearly interpolated between the two values of s/d.

4. Regression-Based Modeling Parameters (MP)

4.1 Relations

Linear regressions using the most influential parameters were conducted to calculate a median estimate for parameters a and b. In a dataset that has a reasonable spread across parameters, a linear regression plane should intersect the data at around the median (i.e., the regression plane should divide the data into two approximately equal groups, with half the data points above and half the data points below the plane). This was found to be the case for this database. Only minor adjustments on the intercept of the regression equations were necessary to achieve a median fit. Regression equations rather than a tabulated format were selected to avoid the problem of stepping functions at parameter boundaries.

Most rectangular columns in the database contained ties with 135^{o} hooks or welded ties with the welded cases accounting for a small minority of tests. Most circular columns in the database were spirally reinforced. A handful of circular columns had welded or core-anchored ties that are considered to perform similar to spirals. In the following, the "spirally" reinforced column group was considered to contain circular columns reinforced with welded circular ties and those with circular ties adequately anchored in the core.

Regression analyses indicated that spirally reinforced circular columns responded differently to variations in influential parameters than rectangular columns reinforced with rectangular ties. To account for such differences, separate regression equations were developed for spirally reinforced circular columns than for all other columns. The most influential parameters for rectangular and circular columns were: the axial load ratio, the transverse reinforcement ratio (ρ_t), and the ratio V_y/V_o. All three parameters are currently used in the standard ASCE 41 to estimate plastic rotation limits for concrete columns. The maximum shear stress applied to a column section is also used in the standard as a parameter to estimate MP. That parameter was not found to have a determining role in column responses analyzed in this work.

The proposed relations between plastic rotations at incipient loss of lateral strength and axial failure are given below. The subscripts R and C in the equations indicate plastic rotations for rectangular and circular columns, respectively. Only relations for b_2 were derived using linear regression because there are too few b_1 values to provide meaningful regression-based estimates.

Plastic rotation capacities for columns other than spirally reinforced circular columns

$$a_R = 0.042 - 0.043\frac{P}{A_g f_c^{'}} + 0.63\rho_t - 0.023\frac{V_y}{V_o} \geq 0.0 \text{ (rad)} \qquad \text{Eq.2}$$

$$b_{2R} = 0.051 - 0.051\frac{P}{A_g f_c^{'}} + 1.3\rho_t - 0.023\frac{V_y}{V_o} \geq a_R \text{(rad)} \qquad \text{Eq.3}$$

Plastic rotation capacities for columns for spirally reinforced circular columns

$$a_C = 0.06 - 0.058\frac{P}{A_g f_c^{'}} + 1.3\rho_t - 0.037\frac{V_y}{V_o} \geq 0.0 \text{ (rad)} \qquad \text{Eq.4}$$

$$b_{2C} = 0.064 - 0.07\frac{P}{A_g f_c^{'}} + 2.85\rho_t - 0.03\frac{V_y}{V_o} \geq a_C \text{(rad)} \qquad \text{Eq.5}$$

When evaluating the above parameters, ρ_t should not be taken greater than 0.0175 and V_y/V_o should not be taken smaller than 0.2. The equation is not applicable for $\rho_t \leq 0.0005$. An upper bound on the transverse reinforcement ratio of 0.0175 is prescribed because few columns in the database contained a ratio exceeding that limit. Equations for modeling parameters cannot be used for columns with a transverse reinforcement ratio below 0.0005 because the equations are not intended for unreinforced columns. A lower limit on V_y/V_o of 0.2 is prescribed because few columns in the database had lower values of V_y/V_o.

Values of a and b_2 for rectangular and spirally reinforced column are presented in Table 1 at practical parameter boundaries. In Table 1, the notation is consistent with that used in Eq. 2 to 5 in which the subscript r is used in reference to rectangular columns while the subscript c is used in reference to circular columns.. As can be observed in the table, for a given set of parameters, spirally reinforced columns exhibited significantly larger deformation capacities than rectangular columns.

Table 1: Values of *a* and *b* at parameter boundaries

P/(A$_g$f'$_c$)	ρ_t	V_y/V_o	a_R (rad)	a_C (rad)	b_{2R} (rad)	b_{2C} (rad)
0	0.0005	0.2	0.038	0.058	0.047	0.060
0	0.0005	2.0	0.0	0.0	0.006	0.005
0	0.0175	0.2	**0.048***	**0.071***	**0.069***	**0.108***
0	0.0175	2.0	0.007	0.0	0.028	0.054
0.7	0.0005	0.2	0.008	0.016	0.011	0.016
0.7	0.0005	2.0	0.0	0.0	0.0	0.0
0.7	0.0175	0.2	0.018	0.029	0.033	0.059
0.7	0.0175	2.0	0.0	0.0	0.0	0.005

* Maximum permissible values

4.2 Analyses of Fit

4.2.1 Estimates of *a*

The cumulative distribution of the error difference between experimental and regression estimates of *a* are plotted for rectangular and circular columns in Fig. 3. Errors are plotted for estimates evaluated using the proposed regression equations as well as for those estimated using the ASCE 41 standard. As can be observed in the figures, the proposed regression equations shifted estimates from conservative ones based on the standard to median estimates; i.e., error = 0 at 0.5 probability of exceedance. For a_R, both methods produced similar spread on the error as evidenced by the similar slopes of the cumulative distribution curves and standard deviations presented in Fig. 3. For a_C however, the proposed relation produced a large shift in estimates from those derived using the standard. This is not surprising given that : 1) the table in the standard defining the *a* values for reinforced concrete columns was based only on data from rectangular column tests [5], and 2) spirally reinforced circular columns in the data set showed increased deformation capacity over rectangular columns with similar parameters.

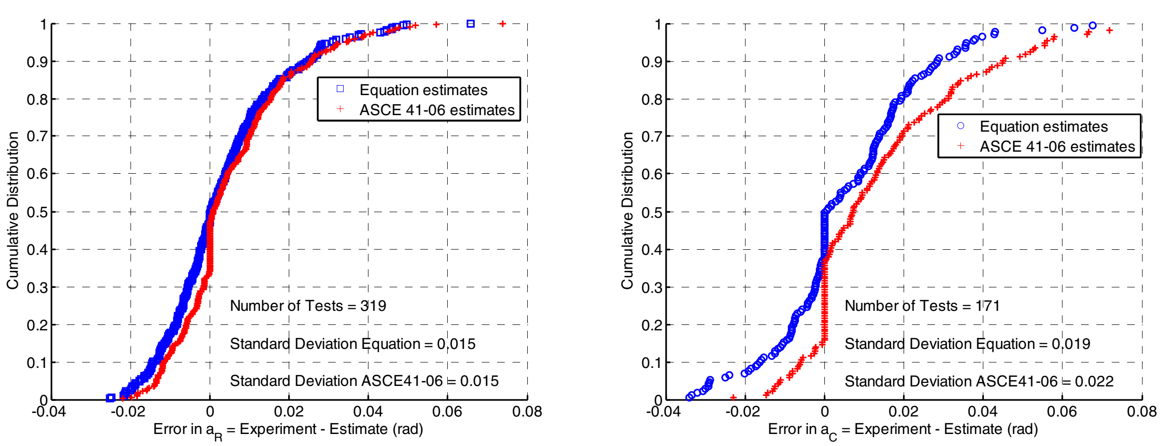

Figure 3: Cumulative distribution of the error between experimental values and estimates for a_R and a_C

The cumulative distribution of the error difference between experimental and regression estimates of a_R are plotted for various bins of rectangular columns in Fig. 4. Test data are divided into bins to illustrate the fit of the proposed relation in various parameter quadrants. As can be observed in the figure, the proposed relation produced estimates that were very close to the median in all bins. Standard deviations on the error of the proposed equation vary from 0.005 to 0.018; which indicates variable accuracy of the proposed equation across bins. Figure 5 presents similar data as Fig. 4 but for circular columns. Similar conclusions can be drawn from Fig. 5 for spirally reinforced circular columns, although the estimates from the proposed equation deviate conservatively from the median estimate for columns with low transverse reinforcement ratio and intermediate values of V_y/V_o (ranging between 0.6 and 1.0). The standard deviations were slightly higher for circular columns than rectangular ones and ranged from 0.005 to 0.029 across bins.

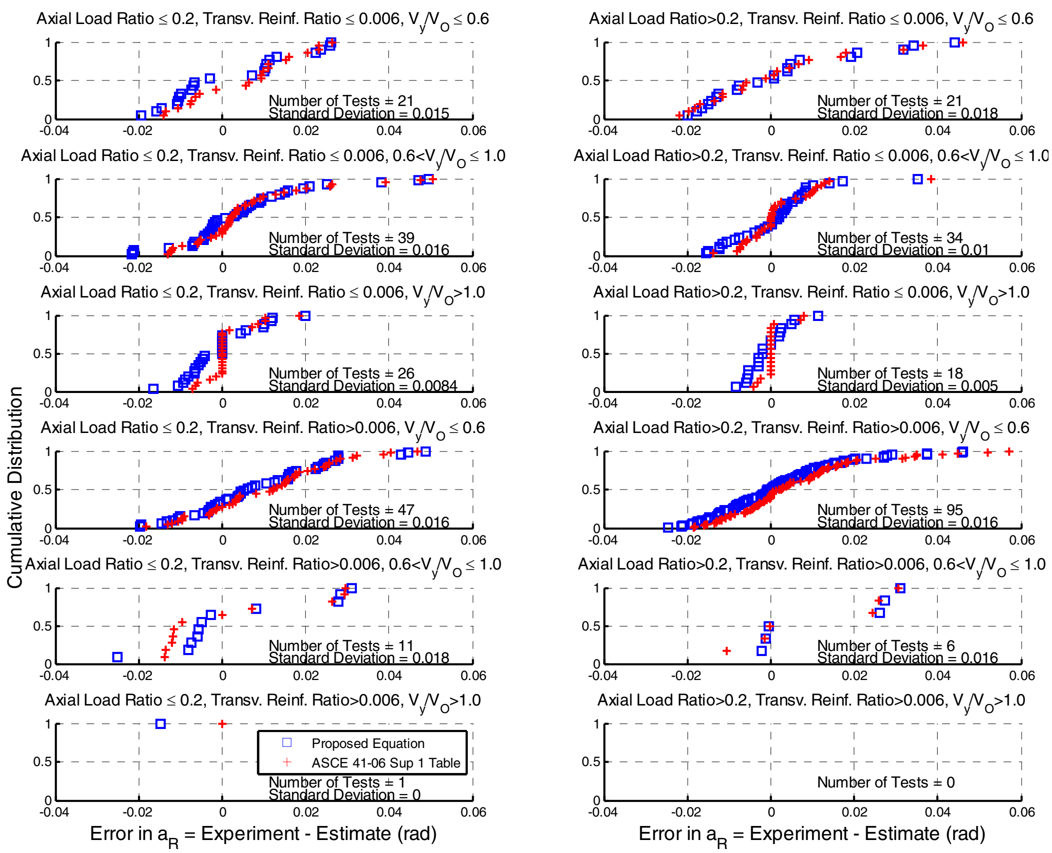

Figure 4: Cumulative distributions of the error between experimental values and estimates for a_R; data split into bins covering various ranges of parameters and standard deviations given for equation estimates only.

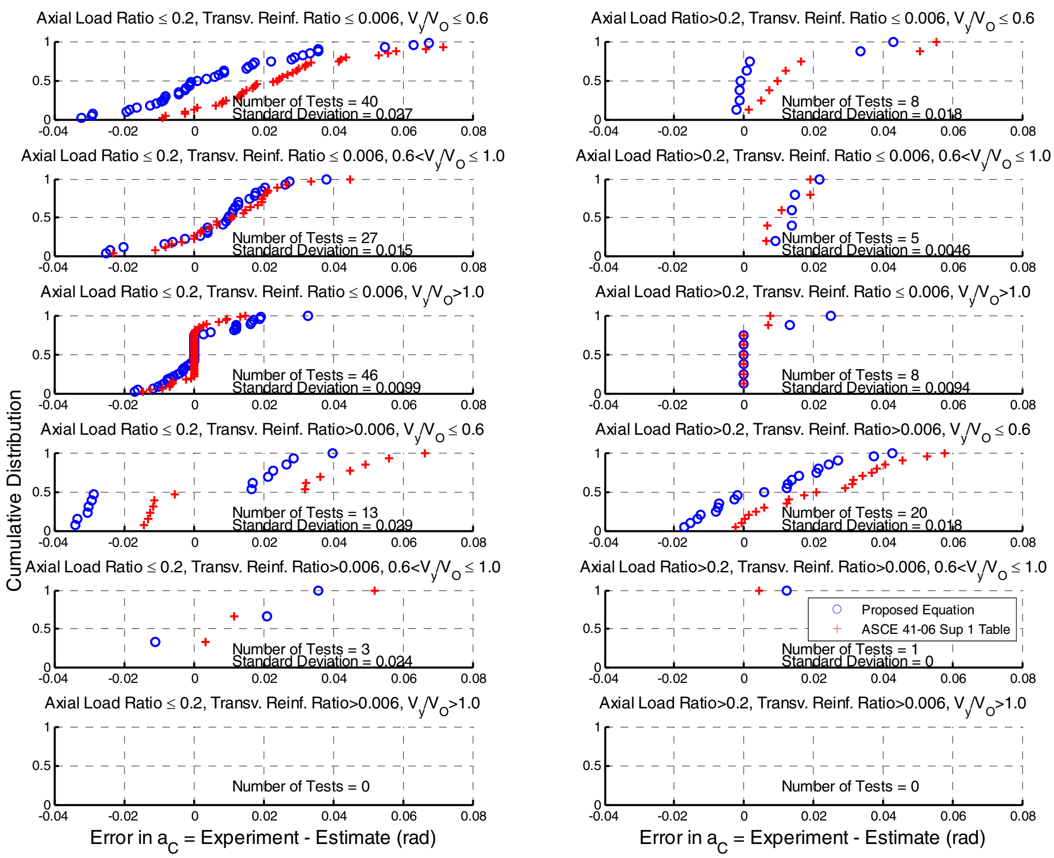

Figure 5: Cumulative distributions of the error between experimental values and estimates for a_C; data split into bins covering various ranges of parameters and standard deviations given for equation estimates only.

The effects of hook details of transverse reinforcement are explored in Fig. 6. In this figure, the error between experimental values and equation-based estimates of a are plotted versus s/d. Rectangular columns with ties having 135° hooks and 90° hooks are highlighted. Columns with unknown hook details are also indicated. Spirally reinforced circular columns as well as those with lapped ties are highlighted. As can be seen in the figure, there appears to be little overall bias in equation estimates with respect to hook details. In fact, for rectangular columns with 90° hooks the median of the error on the estimate of a_R is 0.005 and the associated standard deviation is 0.011, while for 135° hooks the median of the error on the estimate of a_R is zero and the associated standard deviation is 0.015. Similarly, for circular columns with lapped ties the mean error of the estimate of a_C is -0.002 and its associated standard deviation is 0.011, while for spirally reinforced columns the mean error of the estimate of a_C is 0.006 and its associated standard deviation is 0.019. For large s/d ratios (above 0.75) the proposed equation for rectangular columns provided conservative estimates even for columns with ties having 90° hooks; 90% of all data points in that range have conservative estimates of a_R. One should note that columns in the database with lapped ties or ties having 90° hooks had relatively low transverse reinforcement ratios, ρ_t (as is the case typically in older existing buildings). The median ρ_t for rectangular columns with 90° ties is 0.0017, while that for circular columns with lapped ties is 0.0008. At such low reinforcement ratios, the contribution of ties to the overall deformation capacity of columns is relatively low, which may explain the observed insensitivity of estimate errors to hook details of ties.

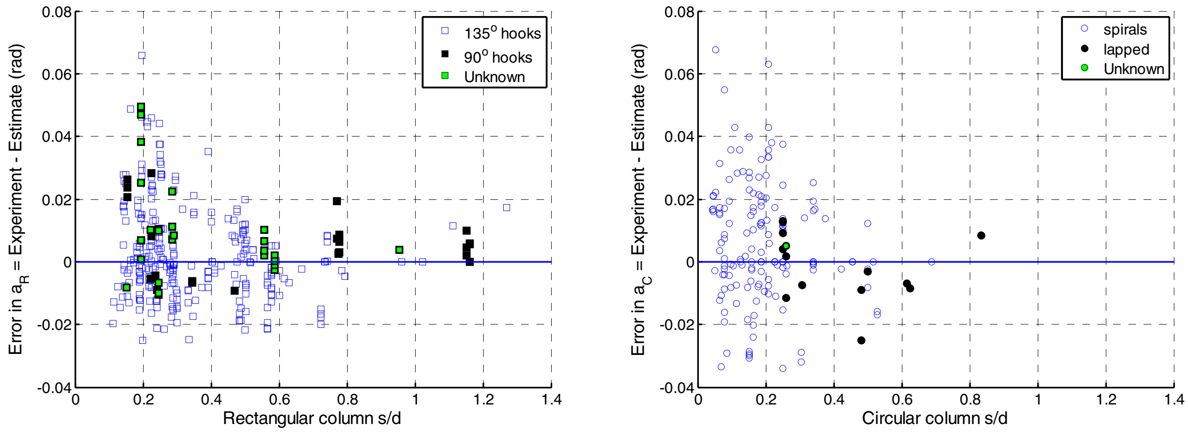

Figure 6: Error between experimental values and equation-based estimates for *a* plotted versus *s/d* with transverse reinforcement type highlighted

4.2.2 Estimates of *b*

The cumulative distribution of the error difference between experimental values and estimates of b_2 are plotted for rectangular and circular columns in Fig. 7. Errors are plotted for estimates evaluated using the proposed regression equations as well as for those estimated using the ASCE 41 standard. The trends observed in Fig. 7 for values of b_2 were similar to those observed for *a* values. It is apparent from Fig. 7 that the proposed regression equations shifted estimates from conservative ones based on the standard to median estimates; i.e., error = 0 at 0.5 probability of exceedance. For b_{2R}, both methods produced similar spread on estimate error as evidenced by the similar slopes of the cumulative distribution curves and the standard deviations. For b_{2C} however, the proposed relation produced a large shift in estimates from those derived using the standard. For brevity, figures similar to Fig. 4 and Fig. 5 are not presented for b_2 values. Similar trends as those for *a* values were observed in the various bins for b_2 values.

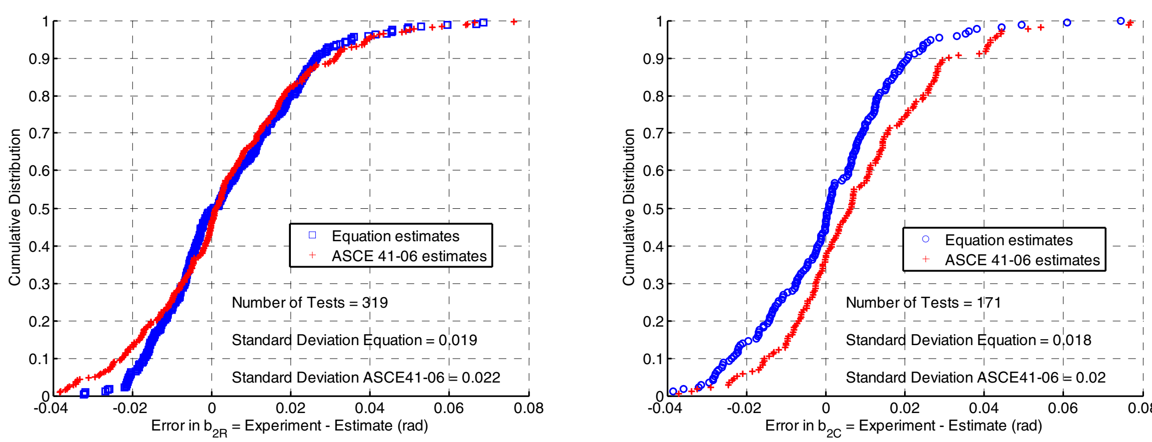

Figure 7: Cumulative distribution of the error between experimental values and estimates for b_{2R} and b_{2C}